ATLAS NOTE
ATLAS-CONF-2016-033
11th July 2016

A re-interpretation of $\sqrt{s} = 8$ TeV ATLAS results on electroweak supersymmetry production to explore general gauge mediated models

The ATLAS Collaboration

Abstract

This document determines the constraints placed by the ATLAS experiment on general gauge mediated (GGM) supersymmetric models. The GGM parameters are chosen in such a way that the constraints from the observed Higgs mass are satisfied. Three varied parameters (μ, M_2 and $\tan\beta$) determine the phenomenology at the LHC, featuring the lightest wino-higgsino mixture neutralinos and charginos decaying to the gravitino and W, Z, Higgs bosons or photons. Constraints from existing ATLAS searches using the full Run 1 dataset of 20.3 fb^{-1} at $\sqrt{s} = 8$ TeV and targeting a variety of final states with multiple leptons or photons are evaluated. Results of different analyses are statistically combined, providing stringent limits on the three theoretical parameters.

ATLAS-CONF-2016-033
11 July 2016

1 Introduction

Supersymmetry (SUSY) [1–6] is a popular theoretical extension to the Standard Model (SM) which postulates an additional symmetry relating fermions and bosons. Each SM particle has a supersymmetric partner with spin which differs by a half. In Gauge Mediated Supersymmetry Breaking (GMSB) [7–9] the SUSY breaking is assumed to occur in a hidden sector, and is communicated to the SUSY sector by gauge fields. This form of SUSY breaking suppresses flavour violating transitions, but allows a large degree of freedom for many masses and scales involved in its formulation. General Gauge Mediated (GGM) [10, 11] models maintain the properties common to all GMSB scenarios whilst avoiding any specifics. The most notable properties of GGM are that the hidden sector decouples from the visible sector as the MSSM couplings approach zero, and that the gravitino $\tilde{G}$ is always the lightest supersymmetric particle (LSP). R-parity[12] is assumed to be conserved, so the LSP is always stable.

This work considers GGM signal scenarios involving light wino-higgsino states with prompt decays. Previous limits placed on GGM models have been applied to scenarios with both electroweak and strong production [13–15], but none have covered the electroweak production of a next-to-lightest-sparticle (NLSP) which is wino-higgsino like. Motivated by the possible final states, the existing ATLAS supersymmetry searches using final states of two photons, two leptons, three leptons and four or more leptons are re-interpreted in these models. These analyses give complementary sensitivity over the explored parameter space and are designed to be orthogonal to facilitate the statistical combination of the results. All results use the full 2012 dataset with 20.3 fb^{-1} of proton-proton collision data at $\sqrt{s}$ =8 TeV. This document begins with a detailed description of the signal models and motivation in Section 2 followed by an overview of the four involved analyses in Section 3. The methods used in re-interpreting these models and the results are presented in Section 4, and finally conclusions are drawn in Section 5.

2 General Gauge Mediated Supersymmetry Breaking Models

The effect of the 125 GeV Higgs boson on phenomenology within GGM models has been explored with extensive scans of the GGM parameter space [16]. Boundaries were set on the GGM parameters, and regions within reach of existing SUSY searches were identified [17]. These results motivate the models considered in this analysis, featuring light neutralinos and charginos and all other sparticles decoupled to 3 TeV. The four other Higgs bosons (H, A, H±) have masses around 2 TeV. Neutralinos and charginos (electroweakinos) are mixtures of the neutral and charged components of the supersymmetric partners to the SM gauge and Higgs fields (the wino, bino and higgsinos). In these models they are wino-higgsino mixtures (not explored by previous ATLAS GGM analyses [13–15]). The bino mass M_1 was set to 1 TeV for the scans, and found to have negligible effects on the results, so is decoupled to 3 TeV to further simplify the models used here. The wino mass M_2 and the higgsino mass parameter μ are both free parameters, and models are considered where one is set to 150 GeV whilst the other is varied from 175 GeV to 800 GeV. The electroweakino mixing is affected by both of these parameters, with the wino component proportional to M_2 and the higgsino component proportional to μ. The masses and mass splittings between the different electroweakinos are also affected. The mass of the lightest neutralino ranges from 98 GeV to 147 GeV. The mass splitting between the lightest chargino and neutralino is around 3 or 4 GeV when μ is fixed to 150 GeV and is less than 1 GeV for the majority of scenarios with M_2 =150 GeV, but increases at small μ = values to 1 and 2 GeV. The parameter $\tan\beta$ defines the ratio of the vacuum expectation values of the two Higgs doublets v_u/v_d, and affects the branching ratios of the electroweakino decays into Higgs bosons. Two sets of scenarios are produced for $\tan\beta$ values of 5 or 20, one with fixed μ and one with fixed M_2, in order to also study the effect of this parameter value on the sensitivity. The masses of the neutralinos and charginos for the scenarios with $\tan\beta$ =20 are on average about 5 GeV higher than those with $\tan\beta$ =5.

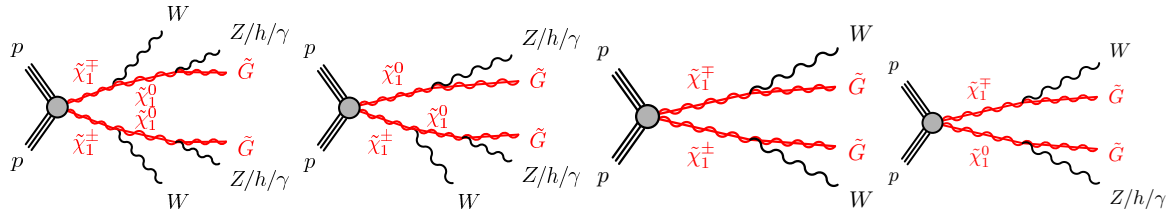

Figure 1: Diagrams illustrating four of the more common processes in the GGM models considered in this analysis.

The production processes contributing to each of the considered scenarios also depend on the parameter values. Production of $\tilde{\chi}_1^{\mp}\tilde{\chi}_1^{\pm}$ and $\tilde{\chi}_1^0\tilde{\chi}_1^{\mp}$ is common for all scenarios and these processes have the highest cross-sections. $\tilde{\chi}_1^{\mp}\tilde{\chi}_2^0$ production is also present for all scenarios with fixed μ, but with a lower cross-section. When μ and M_2 are both relatively low, production modes involving the heavier electroweakinos also contribute with a small fraction, as the sparticle masses are all lower. The subsequent decays of the sparticles predominantly produce W, Z, and Higgs bosons and photons in the final state, motivating a combination of analyses which target multiple leptons or photons. Diagrams showing the most common production and decay processes within these models are displayed in Figure 1. The branching ratios of the electroweakino decays into the different modes depend on all parameter values discussed previously. The wino component of the lightest neutralino allows decays to $\gamma\tilde{G}$ or $Z\tilde{G}$, and the higgsino component can decay to $Z\tilde{G}$ or $h\tilde{G}$. The branching fractions of the lightest neutralino decays for each of the scenarios

considered are summarised in Figure 2, along with the masses of the lightest chargino and neutralino as a function of μ and M_2. The branching ratio to photons decreases with increasing μ or M_2, whilst the branching ratios to decays producing leptons increase. The lightest chargino will decay to the neutralino and either a lepton neutrino pair or quark pair produced via a virtual W boson. The branching ratio to taus is subject to a phase-space effect relating to the chargino-neutralino mass splitting and is suppressed with respect to the electron and muon modes. The differences seen as a function of μ in Figure 3(c) and (e) are directly proportional to the resulting mass splitting between the two lightest electroweakinos. If the mass splitting is too small for decay to the lightest neutralino, the chargino decay will proceed directly to the gravitino and a W boson. This change occurs between μ values of 175 GeV and 300 GeV when M_2 is fixed, and does not occur for the fixed μ scenarios as the mass splittings between electroweakinos are always sufficiently large. This can be seen in Figure 3 showing the branching ratios for the lightest chargino for each of the scenarios considered and the mass splitting between the lightest chargino and neutralino.

The SUSY mass spectra, neutralino and chargino mixing and electroweakino branching ratios were calculated using SuSpect 2.41 [18] and SDECAY 1.3 [19], with the exception of the lightest neutralino and instances where the chargino cannot decay to the neutralino so proceeds directly to a gravitino. These were calculated by Pythia 6 [20] during the event generation to include decays to gravitinos. The lifetime of the sparticles in GGM models is only related to the gravitino mass. This is set to 1 eV for these models, in order to ensure prompt decays detectable by ATLAS. The samples were generated using MadGraph5_aMC@NLOv2.2.2 [21] interfaced with Pythia 6.428 [20], and the signal cross-sections were calculated per subprocess to next-to-leading order in the strong coupling constant using Prospino2 [22]. The nominal cross section and the uncertainty are taken from an envelope of cross section predictions using different PDF sets and factorisation and renormalisation scales, as described in Ref. [23]. The samples are processed with a fast simulation of the ATLAS detector using a parametric response of the electromagnetic and hadronic calorimeters [24] and Geant4 [25] elsewhere. Simulated events are weighted to match the distribution of the mean number of interactions per bunch crossing in data, and are reconstructed in the same manner as data.

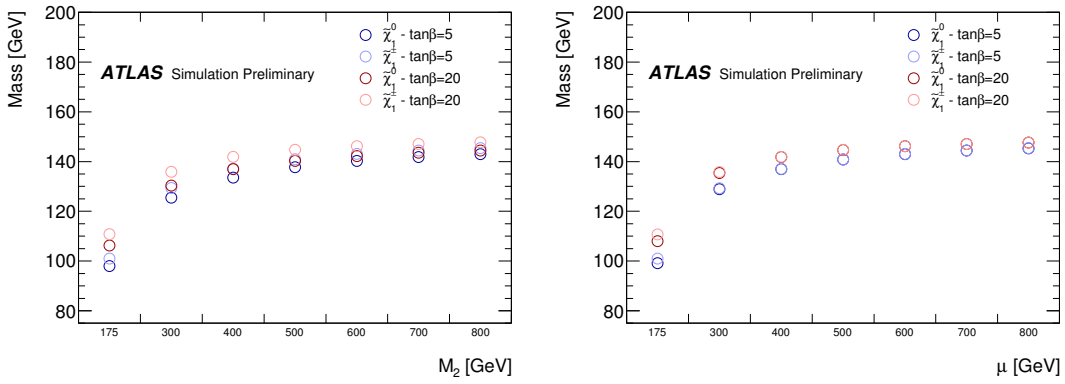

(a) μ=150 GeV (b) M_2=150 GeV

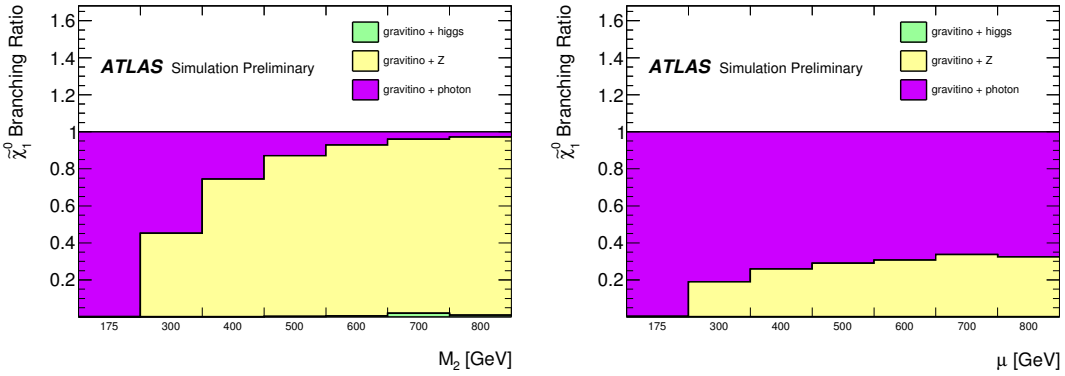

(c) tan β=5, μ=150 GeV (d) tan β=5, M_2=150 GeV

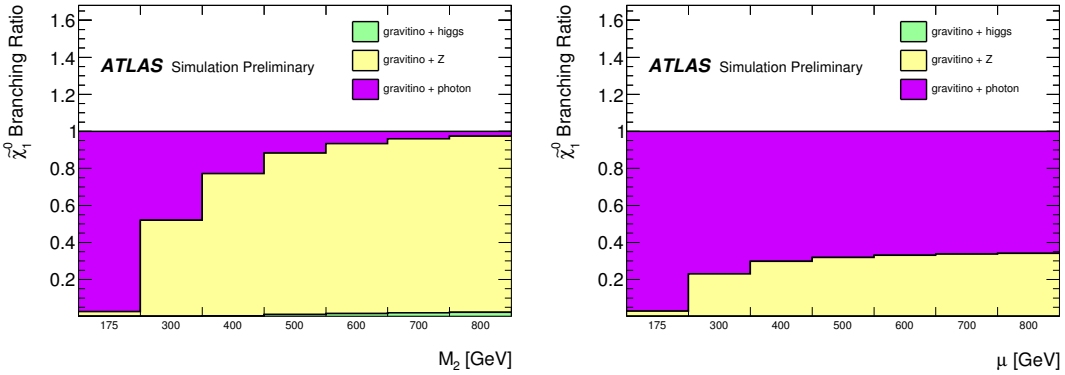

(e) tan β=20, μ=150 GeV (f) tan β=20, M_2=150 GeV

Figure 2: Top two plots display the masses of the lightest neutralino and lightest chargino, on the left as a function of M_2 and on the right as a function of μ for both tan β values. Branching ratios of the $\tilde{\chi}_1^0$ for each of the signal scenarios considered are shown in the four lower plots.

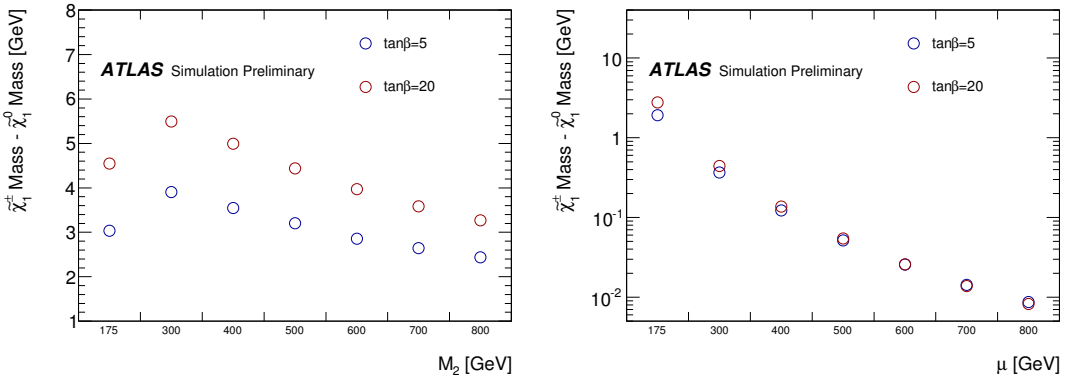

(a) μ=150 GeV (b) M_2=150 GeV

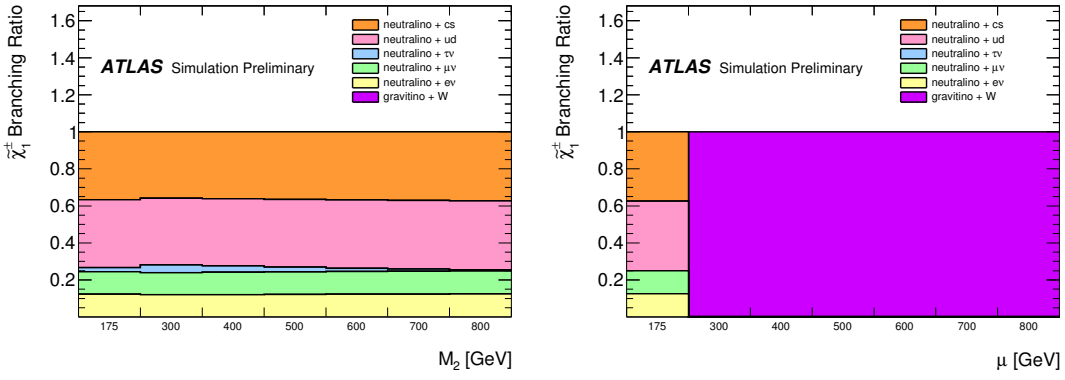

(c) tan β=5, μ=150 GeV (d) tan β=5, M_2=150 GeV

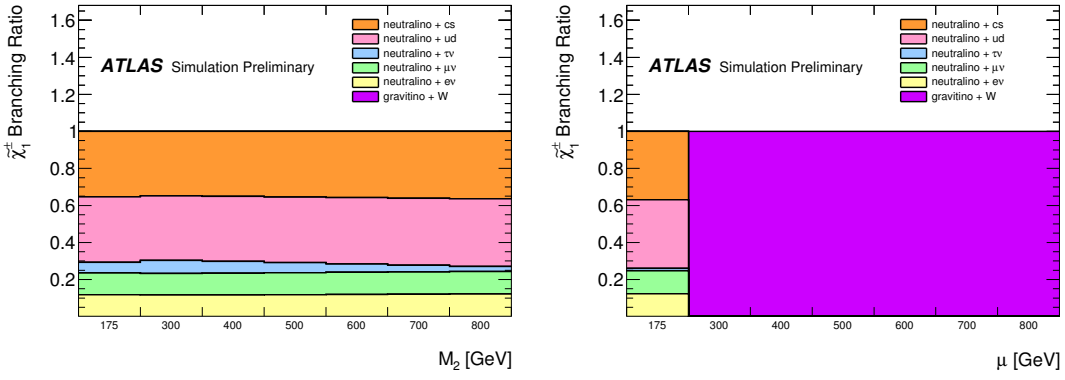

(e) tan β=20, μ=150 GeV (f) tan β=20, M_2=150 GeV

Figure 3: Top two plots display the mass splitting between the lightest neutralino and lightest chargino, on the left as a function of M_2 and on the right as a function of μ for both tan β values. Branching ratios of the $\tilde{\chi}_1^{\pm}$ for each of the signal scenarios considered are shown in the four lower plots.

3 Analyses included in the re-interpretation

Electroweak supersymmetry searches which require two photons, two leptons, three leptons or four or more leptons are sensitive to the models described in Section 2, and re-interpreted to set new exclusion limits. Contributions from SM processes to hadronic final states are much larger, so there is not a good discrimination between signal and background. An outline of each of the included analyses is presented below, and definitions of all signal regions used can be found in Tables 1-4.

- **2γ**: The diphoton analysis looks for events with two photons and large missing transverse energy in the final state. It targets GGM models with light wino- and bino-like electroweakinos and defines several signal regions, two of which (WP1 and WP2) focus on electroweak production. Additional variables used to define these regions include the transverse momentum of jets and angles between the leading photon or leading jet and the missing transverse energy. Details can be found in Ref. [14].
- **2ℓ**: The electroweak two lepton analysis requires exactly two light leptons with opposite charges. Seven signal regions are defined, three targeting slepton pair production and slepton-mediated decays (SR-m$_{T2}$), three targeting the WW-mediated $\tilde{\chi}_1^{\pm}\tilde{\chi}_1^{\mp}$ model (SR-WW) and one targeting the WZ-mediated $\tilde{\chi}_1^{\pm}\tilde{\chi}_2^0$ model (SR-Zjets). Details can be found in Ref. [26].
- **3ℓ**: This analysis requires exactly three leptons (electrons, muons or taus) and defines five signal regions containing 0-2 hadronically decaying taus. These target the $\tilde{\ell}_{\mathrm{L}}$-mediated $\tilde{\chi}_1^{\pm}\tilde{\chi}_2^0$ scenario (SR0τa), the $\tilde{\tau}$-mediated $\tilde{\chi}_1^{\pm}\tilde{\chi}_2^0$ scenario (SR2τa), the WZ-mediated $\tilde{\chi}_1^{\pm}\tilde{\chi}_2^0$ scenario (SR0τa) and the Wh-mediated $\tilde{\chi}_1^{\pm}\tilde{\chi}_2^0$ scenario (SR0τb, SR1τ and SR2τb). Signal region SR0τa selects light leptons and uses twenty bins with varying values of di-lepton invariant mass, missing transverse energy and transverse mass. Details can be found in Ref. [27].
- **4ℓ**: This analysis requires at least four leptons including up to two hadronically decaying taus. Nine signal regions are defined to target R-parity violating models[12] (SR0noZb, SR1noZb and SR2noZb), the $\tilde{\ell}_{\mathrm{R}}$-mediated $\tilde{\chi}_2^0\tilde{\chi}_3^0$ scenario (SR0noZa), the $\tilde{\tau}$-mediated $\tilde{\chi}_2^0\tilde{\chi}_3^0$ scenario (SR1noZa and SR2noZa) and the ZZ-mediated $\tilde{\chi}_2^0\tilde{\chi}_3^0$ scenario (SR0Z), as well as General Gauge mediated scenarios (SR0Z). Details can be found in Ref. [15].

Table 1: Definitions of the two 2γ signal regions used in this analysis. H_{T} is the sum of the magnitudes of the transverse momenta of the photons, leptons and jets in the event [14].

SR	WP1	WP2
Number of photons (E_{T} [GeV])	> 1 (> 75)	> 1 (> 75)
$E_{\mathrm{T}}^{\mathrm{miss}}$ [GeV]	> 150	> 200
H_{T} [GeV]	> 600	> 400
$\Delta\phi_{\mathrm{min}}$(jet, $E_{\mathrm{T}}^{\mathrm{miss}}$) (Number of leading jets)	> 0.5 (2)	> 0.5 (2)
$\Delta\phi_{\mathrm{min}}(\gamma, E_{\mathrm{T}}^{\mathrm{miss}})$	—	> 0.5

Table 2: Definitions of the two 2ℓ signal regions used in this analysis. DF and SF signify same flavour and different flavour lepton pairs, and the criteria on $|m_{ll} - m_Z|$ are applied only to same flavour events. m_{T2} is the stransverse mass variable which relates to the transverse momenta and transverse masses of the two leptons, and $E_T^{miss,rel}$ is the missing transverse energy with a suppression on contributions arising from mismeasurements. Both are defined in Ref. [26].

SR	WWa	WWb
lepton flavour	DF,SF	DF,SF
central light jets	0	0
central b-jets	0	0
forward jets	0	0
$\|m_{ll} - m_Z\|$ [GeV]	> 10	> 10
m_{ll} [GeV]	< 120	< 170
$E_T^{miss,rel}$ [GeV]	> 80	—
p_T^{ll} [GeV]	> 80	—
m_{T2} [GeV]	—	> 90

Table 3: Definitions of the bins used from the 3ℓ signal region SR0τa [27]. m_{SFOS} is the invariant mass of the same-flavour opposite-sign light lepton pair with invariant mass closest to that of the Z boson. The Z veto requires that the invariant mass of the three selected leptons must be more than 10 GeV from the Z boson mass.

SR0τa bin	Flavour/sign	b-jet	m_{SFOS}[GeV]	m_{T}[GeV]	$E_{\mathrm{T}}^{\mathrm{miss}}$[GeV]	Z veto
13	$\ell^+\ell^-\ell$	veto	81.2–101.2	0–110	50–90	yes
14	$\ell^+\ell^-\ell$	veto	81.2–101.2	0–110	>90	no
15	$\ell^+\ell^-\ell$	veto	81.2–101.2	>110	50–135	no

Table 4: Definition of the 4ℓ signal region SR0Z [15]. m_{SFOS} is the invariant mass of the same-flavour opposite-sign light lept on pair with invariant mass closest to that of the Z boson.

	N(ℓ)	m_{SFOS}[GeV]	$E_{\mathrm{T}}^{\mathrm{miss}}$ [GeV]
SR0Z	$\geq$4	81.2–101.2	$>$75

4 Results

Two Photon Analysis

Diphoton events are predominantly produced when both of the lightest neutralinos decay to a photon and a gravitino. The branching fraction for this decreases significantly for the μ =150 GeV scenarios when M_2 is greater than 300 GeV as decays to Z and Higgs bosons become kinematically possible. This is reflected in the signal yields, which are higher for the scenarios at $M1$ =175 GeV and then decrease with increasing M_2. For the M_2 =150 GeV scenarios the diphoton regions have a high sensitivity for the lowest mass point at μ =175 GeV. However, above this μ value they lose sensitivity because the sparticle mass splittings become too small to allow decays from the lightest chargino to the lightest neutralino, and the preferred decay is into a W boson and the gravitino. As production processes including the lightest chargino contribute most, very few events result in two of the lightest neutralinos which can then decay to photons. All scenarios at μ or M_2 =175 GeV are excluded, and good sensitivity for the scenarios with M_2 =150 GeV and μ =300 GeV is shown. As the two regions, WWa and WWb, are not mutually exclusive, the one with the best expected CL_S value is selected for each point.

Two Lepton Analysis

Most of the possible combinations of production and decay processes in these models lead to more than two leptons. For the majority of cases where more than two leptons are produced in the final state, the event will not pass the 2ℓ selection, which requires exactly two leptons. Two leptons are produced in $\tilde{\chi}_1^{\mp}\tilde{\chi}_1^{\pm}$ production where both charginos decay to a W boson and the gravitino, and in processes where one of the final $\tilde{\chi}_1^0\tilde{\chi}_1^0$ pair decays to a Z or Higgs boson and the other decays photonically. The scenarios with fixed M_2=150 GeV and μ >175 GeV have a high $\tilde{\chi}_1^{\mp}\tilde{\chi}_1^{\pm}$ production cross-section and the charginos decay almost exclusively to a W boson plus a gravitino. This is where the 2ℓ signal regions have significant sensitivity, as the signature is almost identical to the one they are designed to target. Harder kinematic requirements become easier to satisfy as the electroweakino masses increase. The signal region WWa [26] is most sensitive for a few low mass scenarios, whilst signal region WWb [26] takes over as μ gets larger. As with the diphoton regions these are not mutually exclusive and so the best expected CL_S value is used to select the region to use for each point.

Three Lepton Analysis

The three lepton signal regions require exactly three leptons, reducing their sensitivity to any processes which result in the production of two leptonically decaying Z bosons. The signal regions used here all require the invariant mass of a same flavour opposite sign lepton pair within 10 GeV of the Z boson mass, making them sensitive to instances where one Z boson is produced. Consequently, as with the two lepton signal regions, significantly less events from the μ=150 GeV scenarios pass the requirements than from the M_2=150 GeV scenarios. Signal region SR0τa-bin13 [27] exhibits a higher signal yield than the other three lepton signal regions for all scenarios, which is expected given that SR0τa-bin14 [27] requires a higher E_T^{miss} and SR0τa-bin15 [27] requires a higher transverse mass. The transverse mass is calculated using the third lepton (not from the same flavour opposite sign pair) and the missing transverse momentum, so will increase as the lightest chargino mass increases. The cross-section decreases as M_2 increases, and the overall effect is relatively unchanging yields for the three lepton regions as a function of M_2. The

bins of the SR0τa [27] 3ℓ signal region are mutually exclusive and so the CL_S values are calculated by statistically combining the results in all three considered bins.

Four Lepton Analysis

The four lepton analysis requires four or more leptons, and the single signal region SR0Z requires two of these to form a same flavour opposite sign pair with an invariant mass within 10 GeV of the Z boson mass. The E_T^{miss} requirement is moderate (75 GeV) and no further kinematic cuts are made, so the region is sensitive to processes resulting in two leptonically decaying Z bosons. Conversely to the two and three lepton regions, this analysis is sensitive to the μ=150 GeV scenarios which have large enough mass splittings for the lightest chargino to always decay to the lightest neutralino, and a much higher branching ratio of the lightest neutralino to Z bosons. More events pass the selection as μ increases despite the falling cross-section, due to the neutralino branching ratio to Z bosons and the electroweakino masses increasing.

4.1 Statistical Interpretation

Using the expected backgrounds and observed data events from the original analyses 95% CL limits can be set on the new signal models. Potential signal contamination in the control regions used to estimate background events in the diphoton analysis is included in the fitting procedure used to produce the exclusion limits. Signal contamination in the control regions of the other analyses is expected to be small. For the two lepton analysis, the contamination predicted for the simplified model process $\tilde{\chi}_1^{\mp}\tilde{\chi}_1^{\pm} \rightarrow W^+W^-\tilde{\chi}_1^0\tilde{\chi}_1^0$ is approximately 10% when the chargino mass is above 100 GeV. The process producing two lepton events in these GGM models is very similar (except that the other decay product is the gravitino not the neutralino) and the lightest chargino is always above 100 GeV, so contributions from these signals should also be small. The background estimation for the three lepton analysis did not rely on control regions, but the expected events were checked against data in validation regions. All of these regions require the E_T^{miss} to be less than 50 GeV, which results in sub-percent level signal contamination for the simplified model processes considered in the three lepton analysis. Again, these differ from the processes in these GGM models because the LSP is the neutralino rather than the gravitino, but the phenomenology is very similar. The four lepton analysis uses control regions which loosen the lepton isolation criteria to estimate contributions from irreducible backgrounds. For the models considered the effect was seen to be negligible in the signal region used here, SR0Z, including for a GGM model with decays via Z bosons. The four lepton events from the GGM models used in this analysis which are selected by the four lepton signal region come from the neutralino decaying to a Z boson, and would not be expected to fail any of the isolation requirements made of the signal leptons.

For the diphoton and two lepton analyses, the best signal region is selected based on the best expected CL_S values, while the three lepton signal regions are statistically combined. Table 5 details which signal regions are used for each of the signal scenarios. All limits are set using the ATLAS HistFitter package [28] (HistFitter-00-00-43). The experimental and theoretical systematic uncertainties on the signal and background samples are modelled within the respective analyses, and correlated if the same systematic uncertainty is present in more than one of the analyses.

Figures 4-7 display the expected and observed limits for each analysis and the combination (either using the best expected analysis or statistically combining more than one). The markers used to plot the combined

Table 5: Signal regions used for each of the signal scenarios. Only regions used for at least one point are included in the table.

Sample μ,M_2,tan β	$\gamma\gamma$ WP1	$\gamma\gamma$ WP2	2ℓ SRWWa	2ℓ SRWWb	3ℓSR0τa	4ℓSR0Z
150,175,5		X				
150,300,5						X
150,400,5						X
150,500,5						X
150,600,5						X
150,700,5						X
150,800,5						X
175,150,5		X				
300,150,5			X		X	
400,150,5			X		X	
500,150,5				X	X	
600,150,5				X	X	
700,150,5				X	X	
800,150,5				X	X	
150,175,20		X				
150,300,20	X					
150,400,20						X
150,500,20						X
150,600,20						X
150,700,20						X
150,800,20						X
175,150,20		X				
300,150,20				X	X	
400,150,20				X	X	
500,150,20				X	X	
600,150,20				X	X	
700,150,20				X	X	
800,150,20				X	X	

or best exclusion limit denote which regions have been used for each point. The resulting combined CL_S values are presented as a function of the wino or higgsino mass parameters, μ or M_2, for two tan β values in Figures 8-11. In Figures 8 and 10 the shape of the excluded cross-section can be understood in terms of the contributions from the diphoton and four lepton analyses. At low mass the diphoton analysis has a strong sensitivity, which decreases at the M_2 =300 GeV scenarios and is negligible at higher masses due to the lower branching ratio to photons from the lightest neutralino. At M_2 =300 GeV the four lepton analysis also has some sensitivity, and a statistical combination of the two regions would be optimal, but suffered from technical difficulties. As a result the best expected CL_S values are used to select either the four lepton or one of the diphoton signal regions for this point. At M_2 =400 GeV the diphoton analysis no longer has any sensitivity, but the mass of the lightest neutralino is still too low to produce an on-shell Z boson and the 75 GeV of missing transverse energy required by 4ℓ SR0Z. This becomes much more likely as M_2 increases, and the sensitivity improves again. This crossover in sensitivity of the analyses can be seen clearly in Figures 4 and 6.

The CL_S is less dependent on the varied parameter for the scenarios with M_2 =150 GeV shown in Figures 9 and 11. This is because the diphoton regions are only sensitive to the lowest mass scenarios, and do not contribute to the statistical combination above this mass. The statistical combination of the 2ℓ and 3ℓ regions from μ =300 GeV improves the exclusion limit, which increases slightly as the sparticles become

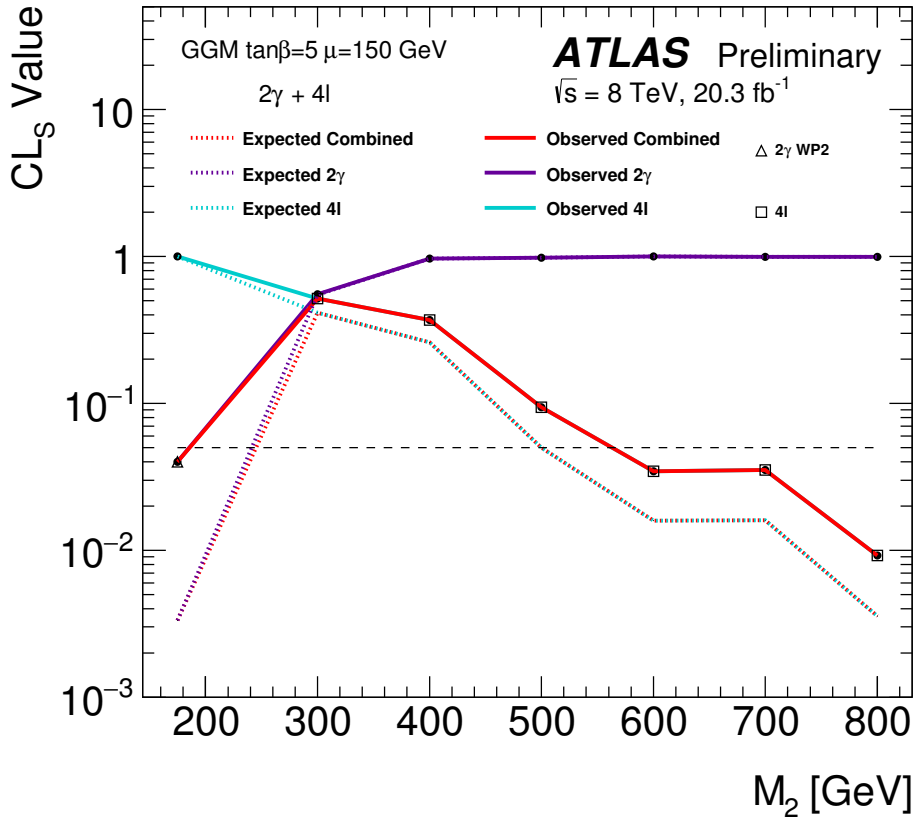

Figure 4: CL_S values for the scenarios with fixed μ and $\tan\beta$ =5 as a function of M_2. The diphoton and four lepton limits are shown separately alongside the combined limit. The markers displayed on the combined limit denote which regions have been used to produce it.

more massive and both analyses become more sensitive. The masses of the electroweakinos are higher for all these scenarios than for the corresponding μ =150 GeV scenarios and therefore the final states more easily satisfy harder kinematic cut criteria. It is clear from Figures 5 and 7 that the diphoton analysis loses sensitivity very quickly as μ increases and the two and three lepton analyses both contribute above μ =175 GeV.

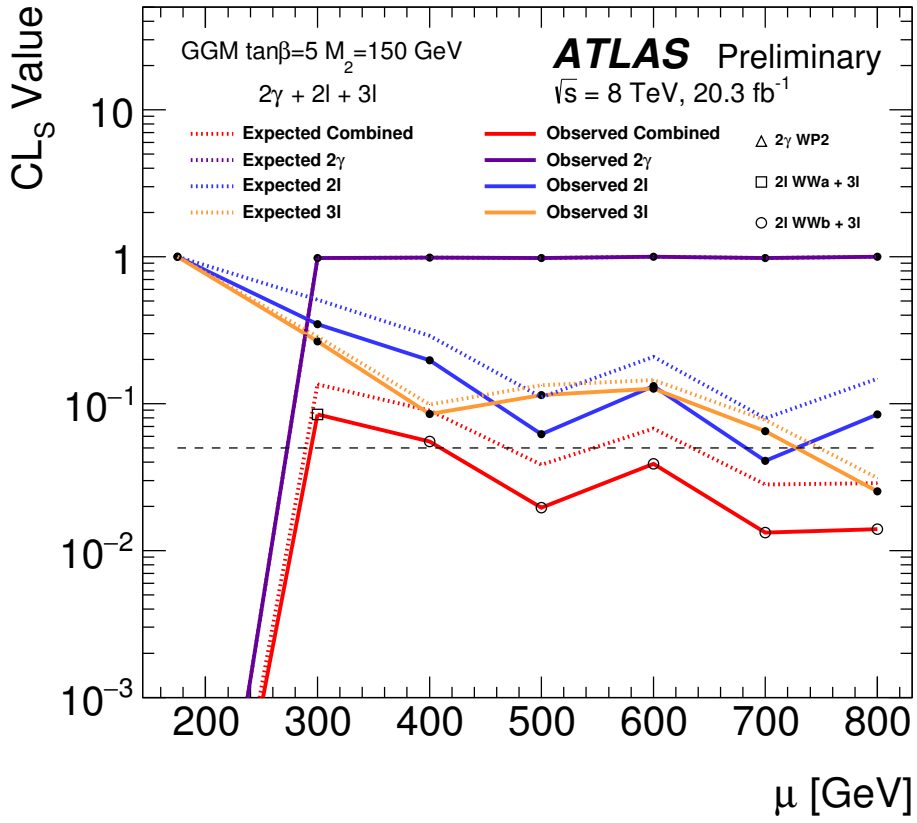

Figure 5: CL_S values for the scenarios with fixed M_2 and $\tan\beta$ =5 as a function of μ. The diphoton, two lepton and three lepton limits are shown separately alongside the combined limit. The markers displayed on the combined limit denote which regions have been used to produce it.

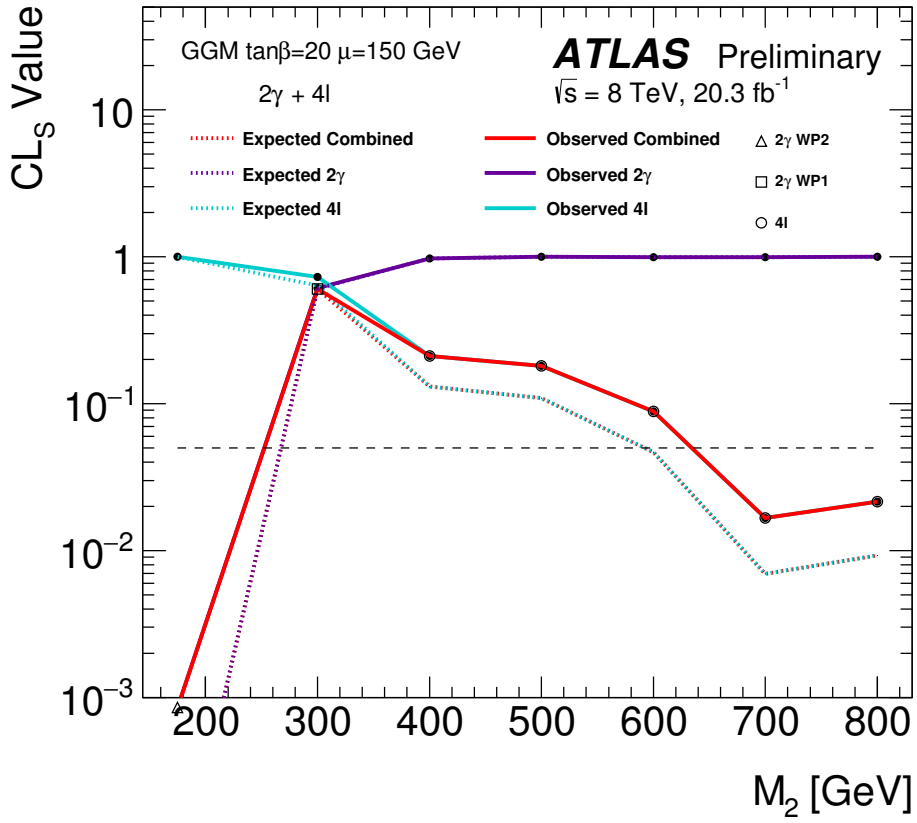

Figure 6: CL_S values for the scenarios with fixed μ and $\tan\beta$ =20 as a function of M_2. The diphoton and four lepton limits are shown separately alongside the combined limit. The markers displayed on the combined limit denote which regions have been used to produce it.

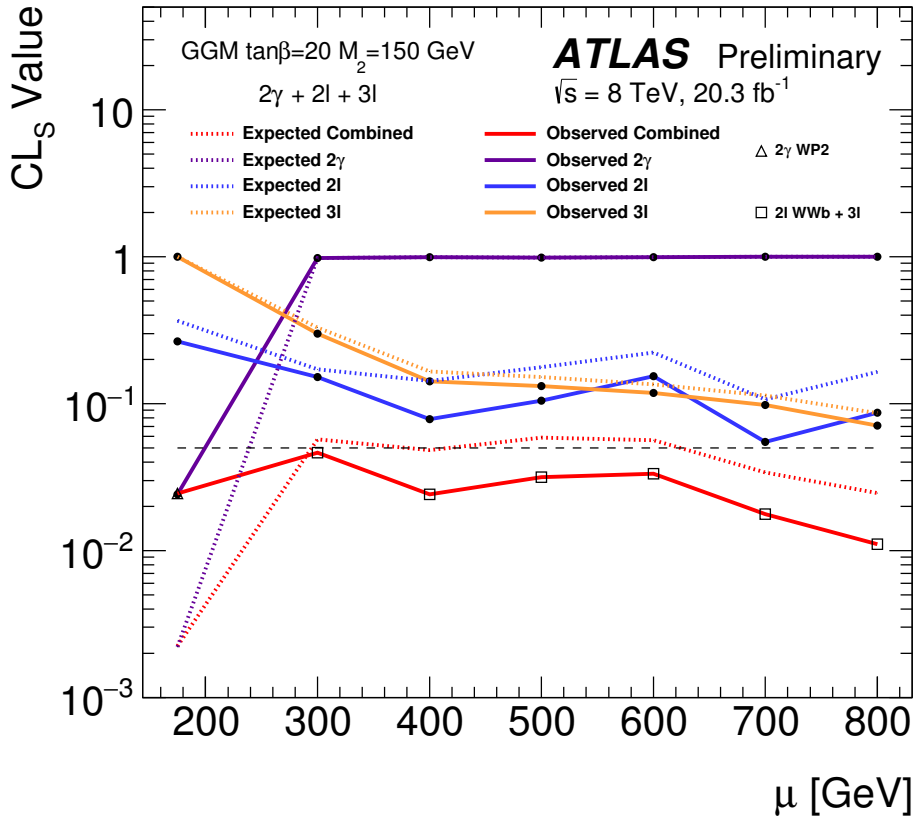

Figure 7: CL_S values for the scenarios with fixed M_2 and $\tan\beta$ =20 as a function of μ. The diphoton, two lepton and three lepton limits are shown separately alongside the combined limit. The markers displayed on the combined limit denote which regions have been used to produce it.

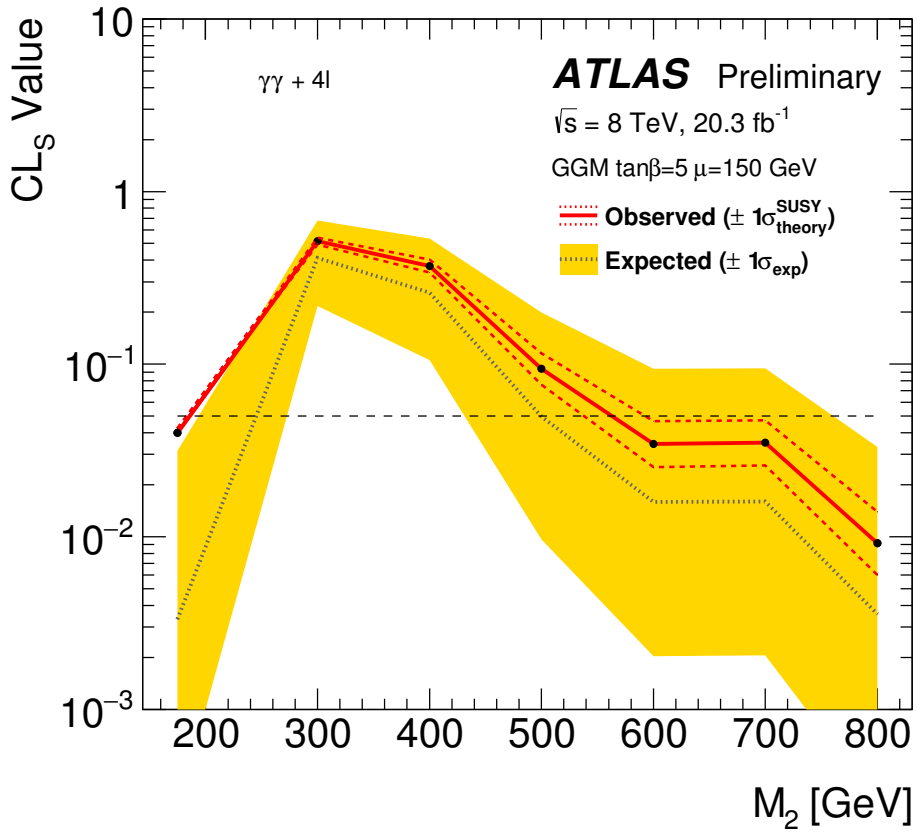

Figure 8: CL$_S$ values for the scenarios with fixed μ and tan β =5 as a function of M_2.

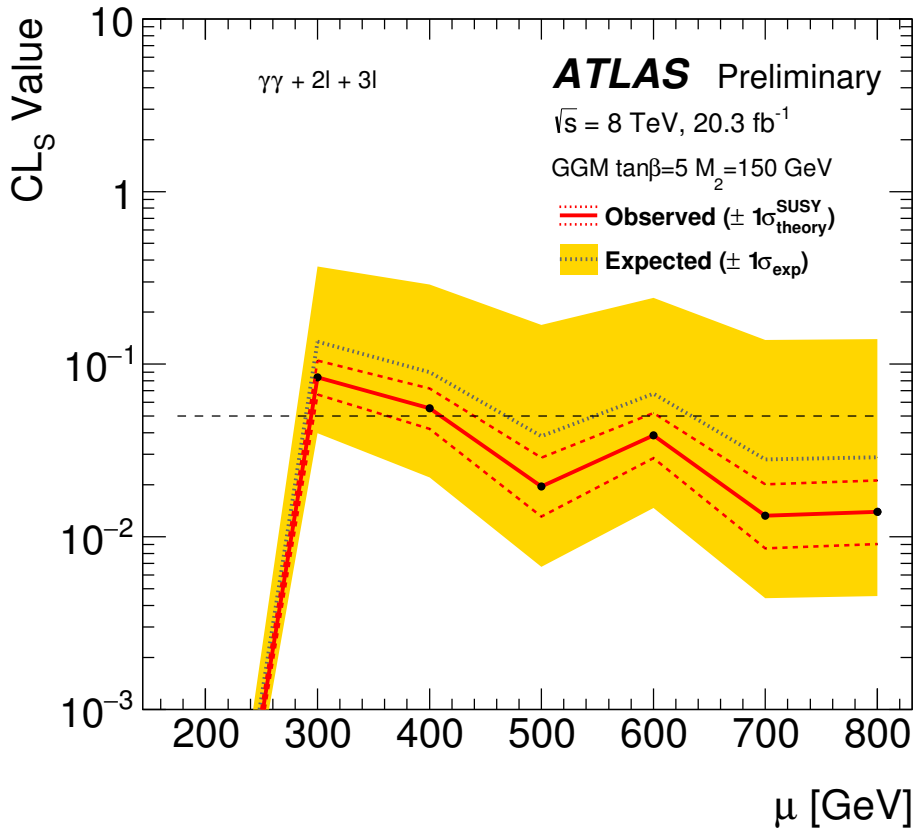

Figure 9: CL$_S$ values for the scenarios with fixed M_2 and tan β =5 as a function of μ.

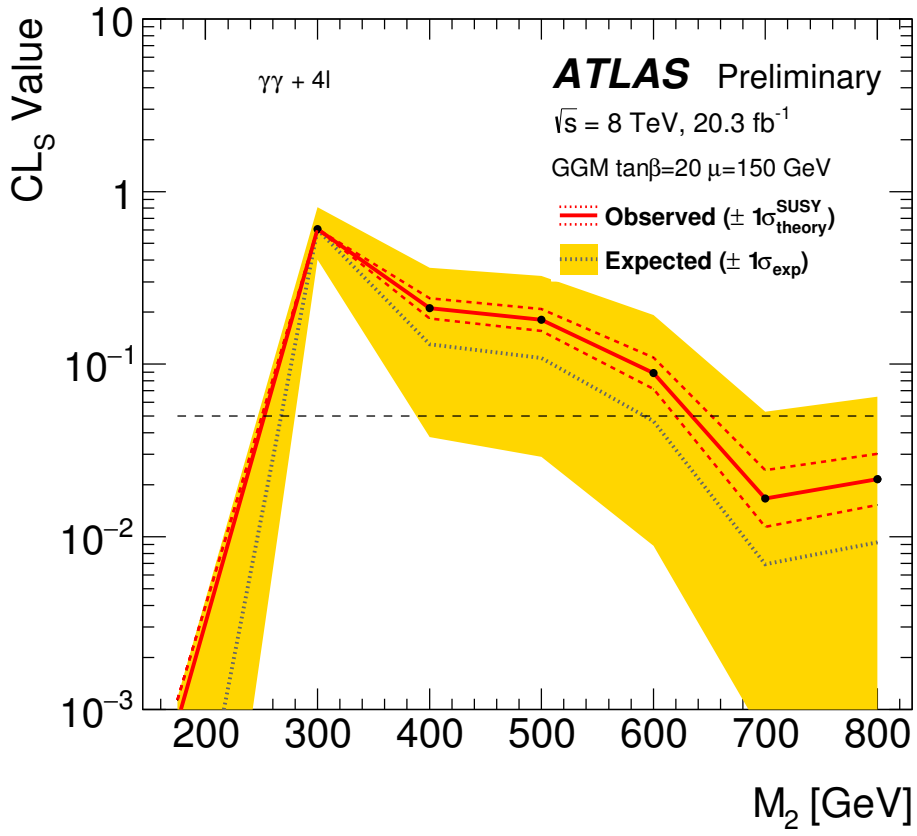

Figure 10: CL$_S$ values for the scenarios with fixed μ and tan β =20 as a function of M_2.

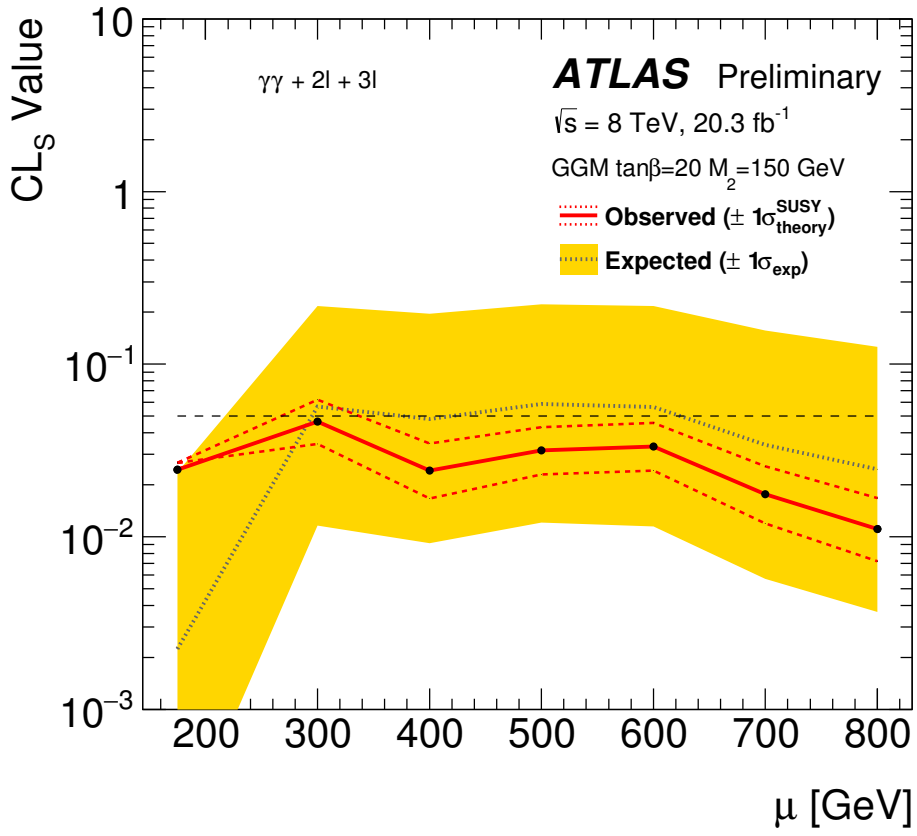

Figure 11: CL$_S$ values for the scenarios with fixed M_2 and tan β =20 as a function of μ.

5 Conclusions

Results are presented on general gauge mediated models consistent with a 125 GeV Higgs boson, which contain light wino-higgsino mixture neutralinos and charginos. They are obtained by statistically combining results from four Run 1 electroweak supersymmetry searches with photons or light leptons in the final state. Model parameters are varied to give a range of branching ratios and mass splittings of these electroweakinos, with final states containing photons and multiple leptons in addition to gravitinos. CLs values are presented either as a function of the wino or higgsino mass parameters, μ or M_2, for two different tan β values of 5 and 20. The most stringent limits are set on models with fixed M_2 =150 GeV, where μ values of 175 GeV and 500 GeV and above are excluded for tan β =5 and μ values of 175 GeV and 400 GeV and above for tan β =20. For models with μ =150 GeV M_2 values of 175 GeV and 600 GeV and above are excluded for the tan β =5 case and 175 GeV and 700 GeV and above for the tan β =20 case. The results motivate a dedicated effort to probe these models in Run 2 more thoroughly, in particular to target μ and M_2 values around 300–500 GeV where leptons are still produced but exclusion was not possible with the existing search regions.

References

[1] Yu. A. Golfand and E. P. Likhtman,
Extension of the Algebra of Poincare Group Generators and Violation of P Invariance,
JETP Lett. **13** (1971) 323, [Pisma Zh. Eksp. Teor. Fiz.13,452(1971)].

[2] D. V. Volkov and V. P. Akulov, *Is the Neutrino a Goldstone Particle?*, Phys. Lett. B **46** (1973) 109.

[3] J. Wess and B. Zumino, *Supergauge Transformations in Four-Dimensions*,
Nucl. Phys. B **70** (1974) 39.

[4] J. Wess and B. Zumino, *Supergauge Invariant Extension of Quantum Electrodynamics*,
Nucl. Phys. B **78** (1974) 1.

[5] S. Ferrara and B. Zumino, *Supergauge Invariant Yang-Mills Theories*,
Nucl. Phys. B **79** (1974) 413.

[6] A. Salam and J. A. Strathdee, *Supersymmetry and Nonabelian Gauges*,
Phys. Lett. B **51** (1974) 353.

[7] M. Dine and W. Fischler,
A Phenomenological Model of Particle Physics Based on Supersymmetry,
Phys. Lett. B **110** (1982) 227.

[8] L. Alvarez-Gaume, M. Claudson and M. B. Wise, *Low-Energy Supersymmetry*,
Nucl. Phys. B **207** (1982) 96.

[9] C. R. Nappi and B. A. Ovrut, *Supersymmetric Extension of the SU(3) x SU(2) x U(1) Model*,
Phys. Lett. B **113** (1982) 175.

[10] C. Cheung, A. L. Fitzpatrick and D. Shih, *(Extra)ordinary gauge mediation*, JHEP **07** (2008) 054,
arXiv: 0710.3585 [hep-ph].

[11] P. Meade, N. Seiberg and D. Shih, *General Gauge Mediation*,
Prog. Theor. Phys. Suppl. **177** (2009) 143, arXiv: 0801.3278 [hep-ph].

[12] G. R. Farrar and P. Fayet, *Phenomenology of the Production, Decay, and Detection of New Hadronic States Associated with Supersymmetry*, Phys. Lett. B **76** (1978) 575.

[13] ATLAS Collaboration,
Search for supersymmetry in events containing a same-flavour opposite-sign dilepton pair, jets, and large missing transverse momentum in $\sqrt{s} = 8$ *TeV pp collisions with the ATLAS detector*,
Eur. Phys. J. C **75** (2015) 318, arXiv: 1503.03290 [hep-ex].

[14] ATLAS Collaboration, *Search for photonic signatures of gauge-mediated supersymmetry in* 8 *TeV pp collisions with the ATLAS detector*, Phys. Rev. D **92** (2015) 072001,
arXiv: 1507.05493 [hep-ex].

[15] ATLAS Collaboration, *Search for supersymmetry in events with four or more leptons in* $\sqrt{s} = 8$ *TeV pp collisions with the ATLAS detector*, Phys. Rev. D **90** (2014) 052001,
arXiv: 1405.5086 [hep-ex].

[16] S. Knapen, D. Redigolo and D. Shih, *General Gauge Mediation at the Weak Scale*, (2015),
arXiv: 1507.04364 [hep-ph].

[17] S. Knapen and D. Redigolo, *Gauge Mediation at LHC: status and prospects*, (2016),
arXiv: 1606.07501 [hep-ph].

[18] A Djouadi, J.-L. Kneur and G Moultaka,
SuSpect: A Fortran code for the Supersymmetric and Higgs particle spectrum in the {MSSM},
Computer Physics Communications **176** (2007) 426 , ISSN: 0010-4655,
URL: http://www.sciencedirect.com/science/article/pii/S001046550600419X.

[19] M. Muhlleitner, A. Djouadi and Y. Mambrini,
SDECAY: A Fortran code for the decays of the supersymmetric particles in the MSSM,
Comput. Phys. Commun. **168** (2005) 46, arXiv: hep-ph/0311167 [hep-ph].

[20] T. Sjostrand, S. Mrenna and P. Z. Skands, *PYTHIA 6.4 Physics and Manual*,
JHEP **0605** (2006) 026, arXiv: hep-ph/0603175.

[21] J. Alwall et al., *The automated computation of tree-level and next-to-leading order differential cross sections, and their matching to parton shower simulations*, JHEP **1407** (2014) 079,
arXiv: 1405.0301 [hep-ph].

[22] W. Beenakker et al., *Squark and gluino production at hadron colliders*,
Nucl.Phys. **B492** (1997) 51, arXiv: hep-ph/9610490 [hep-ph].

[23] M. Kramer et al., *Supersymmetry production cross sections in pp collisions at* $\sqrt{s} = 7$ *TeV*, (2012),
arXiv: 1206.2892 [hep-ph].

[24] ATLAS Collaboration,
The simulation principle and performance of the ATLAS fast calorimeter simulation FastCaloSim,
ATL-PHYS-PUB-2010-013 (2010), URL: http://cdsweb.cern.ch/record/1300517.

[25] S. Agostinelli et al., *GEANT4: A simulation toolkit*, Nucl. Instrum. Meth. **A 506** (2003) 250.

[26] ATLAS Collaboration,
Search for direct production of charginos, neutralinos and sleptons in final states with two leptons and missing transverse momentum in pp collisions at $\sqrt{s} = 8$ *TeV with the ATLAS detector*,
JHEP **1405** (2014) 071, arXiv: 1403.5294 [hep-ex].

[27] ATLAS Collaboration,
Search for direct production of charginos and neutralinos in events with three leptons and missing transverse momentum in $\sqrt{s} = 8$ *TeV pp collisions with the ATLAS detector*,
JHEP **1404** (2014) 169, arXiv: 1402.7029 [hep-ex].

[28] M. Baak et al., *HistFitter software framework for statistical data analysis*,
Eur. Phys. J. **C75** (2015) 153, arXiv: 1410.1280 [hep-ex].